

ROBUSTNESS OPTIMISATION OF AEROCAPTURE TRAJECTORY DESIGN USING A HYBRID CO-EVOLUTIONARY APPROACH

Massimiliano Vasile

Department of Aerospace Engineering
Politecnico di Milano, via La Masa 34, 20156, Milano, Italy
vasile@aero.polimi.it

ABSTRACT

This paper presents an approach to the robust design of space trajectories in which uncertainty in both spacecraft subsystems and trajectory parameters play an important role. Both aleatory and epistemic uncertainties are considered and represented by evidence theory. The optimisation is then performed with a novel hybrid coevolutionary algorithm. This methodology is applied to the design of aerocapture trajectories on Mars. Some interesting results will be presented.

1. INTRODUCTION

Many design problems, in aerospace engineering, are characterised by a certain level of uncertainties especially in the early phase of the design. This is particularly true for aerocapture manoeuvres since the result of the atmospheric pass is sensitive to a number of different parameters (ballistic coefficient, entry velocity, lift-to-drag ratio, atmospheric density, etc...), associated to different disciplines (structures, aerodynamics, mission analysis, etc...), which in general are not completely defined (epistemic uncertainty) or are subject to stochastic variations (aleatory uncertainty). Not only are these design problems affected by uncertainties but often they are also aiming at minimising a number of different objectives of different nature at the same time with a consequent coupling of the effects of uncertainties associated to the computation of each objective. Therefore it would be desirable, especially in the early phase of the design, to compute solutions which are robust with respect to uncertainties, by minimising the associated dispersion, and deriving an index of reliability of the obtained solutions. In recent times, robustness optimisation or reliability enhancement techniques have received a growing interest in multidisciplinary design and optimisation (MDO)[1,2,3] and can represent a promising tool also in mission analysis and design.

In this paper, an approach based on a hybridisation of a branching technique with co-evolutionary algorithms[8,9], is proposed for the search of solutions that are robust to uncertainties.

Here both aleatory and epistemic uncertainties are taken into account using evidence theory[1].

Robustness is expressed as the confidence or *belief* in the goal attained and in the satisfaction of the constraints. The expected values of the goals are optimised while maximising at the same time the associated confidence. The value of the belief in the expected results is computed from the basic belief assigned to the intervals containing the expected value of the uncertain parameters. The branching technique is then used to partition the domain of each design parameter into subdomains and on each subdomain a co-evolutionary algorithm is executed in order to find a set of Pareto optimal solutions. By iterating alternatively branching and co-evolution the algorithm eventually converges to a subset of the Pareto front. In order to automatically select a limited set of robust solutions among all Pareto optimal ones, only optimal compromise among goals and associated confidence are kept.

The use of a global search approach with no requirements on the continuity and differentiability of the functions overcome the problems encountered by MDO approaches, based on gradient methods, that make use of evidence theory[2]. Furthermore the hybrid branching/co-evolution will provide a characterisation of the reliability of the solutions bounding the expected values within a confidence interval.

The proposed multiobjective optimisation is then applied to the design of aerocapture trajectories characterised by uncertainties on atmospheric density, shape, L/D coefficient and thermal properties of the spacecraft. The aim is to maximise the mass of the payload, minimising peak heat flow and maximising the entry corridor width.

2. REPRESENTATION OF UNCERTAINTY

It is a common habit in reliable design to classify uncertainty, whether it occurs in input parameters or in system model, into *aleatory* uncertainty and *epistemic* uncertainty. The former is also referred to as variability, irreducible uncertainty or stochastic uncertainty, while the latter is also referred to as reducible uncertainty or uncertainty due to a lack of knowledge. In order to correctly treat both kinds of uncertainty in a consistent computational framework for system engineering several authors have recently proposed the use of evidence theory[1,2,3]. Evidence theory, born with Dempster and Shafer in the '70, can be seen as a generalisation of probability and possibility theory. In

the following we will use the notation presented in the work of Oberkampf and Helton[1].

Similar to probability theory, the evidence theory representation for the uncertainty in the design vector \mathbf{x} is built up from the representation for the uncertainty in the components of \mathbf{x} . Typically, in the early phase of the design process, specialists have a poor knowledge of some design parameters, therefore they express a *guess*. This guess is here represented by sets ε of values a parameter can assume and a basic probability (BPA) $m(\varepsilon)$ is assigned to each set such that (i) $m(\emptyset)=0$ and (ii) $\sum_{\varepsilon \in \Theta} m(\varepsilon)=1$, where Θ is the set collecting all possible ε and unions of ε . The BPA for \mathbf{x} is computed with the simplifying assumption that there are no correlations or restrictions involving the components of \mathbf{x} . Unlike probability theory that uses a single value as the only representation for uncertainty, evidence theory uses two values: the belief Bel and the plausibility Pl defined as follows:

$$Bel_y(Y_v) = Bel_p(f^{-1}(Y_v)) = \sum_{j \in I_B} m_p(U_j) \quad (1)$$

$$Pl_y(Y_v) = Pl_p(f^{-1}(Y_v)) = \sum_{j \in I_p} m_p(U_j) \quad (2)$$

where the two index sets I_B and I_p are defined as:

$$\begin{aligned} I_B &= \{j : U_j \subset f^{-1}(Y_v)\} \\ I_p &= \{j : U_j \cap f^{-1}(Y_v) \neq \emptyset\} \end{aligned} \quad (3)$$

the set Y_v is defined as:

$$Y_v = \{y : y = f(\mathbf{x}) > v, \mathbf{x} \in D\} \quad (4)$$

and $U \subset D$. Each possible value for y is then given by all possible values assumed by the components of \mathbf{x} within the subsets ε . The resulting BPAs for the product space D of the subsets ε , is given by the Cartesian product $\varepsilon_1 \times \varepsilon_2 \times \dots \times \varepsilon_n$ of the subset of the components of \mathbf{x} :

$$m_p(\varepsilon) = \begin{cases} \prod_{i=1}^p m_i(\varepsilon_i) & \text{if } \varepsilon_i \subset A_i \text{ and } \varepsilon = \varepsilon_1 \times \varepsilon_2 \times \dots \times \varepsilon_p \\ 0 & \text{otherwise} \end{cases} \quad (5)$$

3. DYNAMIC MODEL

The aerocapture manoeuvre is generally composed of two phases: an atmospheric phase and an orbital phase. The orbital phase before the atmospheric phase is propagated analytically from the arrival point on the sphere of influence to the entry point in the atmosphere. The atmospheric phase is then propagated numerically

using the following two dimensional set of differential equations (see Fig.1):

$$\dot{r} = v_r; \quad \dot{v}_r = -\frac{\mu}{r^2} + \frac{v_\theta^2}{r} + f_d \cos \beta + f_l \sin \beta \quad (6)$$

$$\dot{\theta} = \frac{v_\theta}{r}; \quad \dot{v}_\theta = -\frac{v_\theta v_r}{r} + f_d \sin \beta + f_l \cos \beta$$

Aerodynamic forces f_d and f_l are modelled as follows:

$$\begin{aligned} f_d &= \frac{1}{2} \rho(H, h) \frac{S}{m} C_d(\alpha, C_{d0}) v^2 \\ f_l &= \frac{1}{2} \rho(H, h) \frac{S}{m} C_l(C_d) v^2 \end{aligned} \quad (7)$$

where α is the angle of attack at the entrance of the atmosphere and is considered constant during the entire atmospheric phase, C_{d0} is the drag at zero angle of attack, S the reference surface of the spacecraft and m its mass. Here the atmospheric density ρ follows an exponential profile function of the altitude h parametrised in the density scale height H . A simplified model is used for the drag and lift coefficients:

$$C_d = C_{d0} + k_1 \alpha^2 \quad \text{with} \quad C_l = \left(\frac{C_d - C_{d0}}{k_2} \right)^{k_3} \quad (8)$$

where k_1 , k_2 and k_3 have been taken equal to 0.00047, 3.2 and 0.4 respectively, in order to fit tabulated data [6,7] for a conic shape re-entry vehicle (see Fig.2).

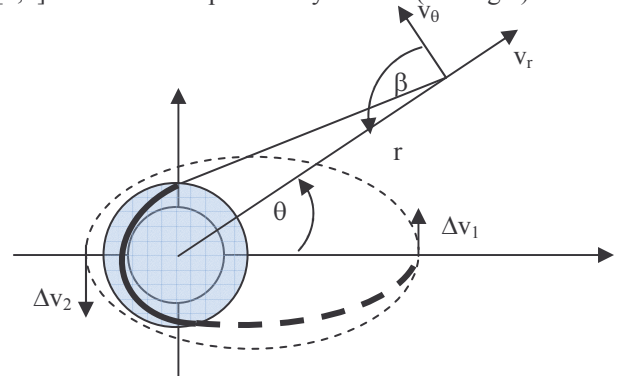


Fig. 1. Cartoon of the trajectory model

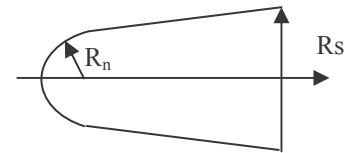


Fig. 2. Cartoon of the Spacecraft model

4. PROBLEM FORMULATION

Due to the high sensitivity related to aerocapture manoeuvres an optimal design of the associated trajectory would require a high accuracy in initial

conditions and spacecraft aerodynamic properties. It is common use to analyse the problem looking at the width of the entry corridor, i.e. the interval of entry angles for which the exit orbital parameters are as desired, while maintaining the maximum g-load and heat flux under a given threshold[4]. This implies some control capabilities of the spacecraft during the atmospheric phase. In this paper we tackle the problem from a different perspective. In case the control is limited or unknown, the spacecraft design should be as such to allow aerocapture even for uncertain parameters and initial conditions. Post atmospheric conditions are then corrected with two Δv manoeuvres, at the apocentre and at the pericentre of the orbit resulting from the aeromanoeuvre. The problem can be generally formulated as follows:

$$\begin{aligned} \min_{\mathbf{x} \in D} \mathbf{F}(\mathbf{x}) \\ q(\mathbf{x}) \leq q_{\max} \\ n(\mathbf{x}) \leq n_{\max} \end{aligned} \quad (9)$$

where \mathbf{F} is an objective function vector dependent on the design vector \mathbf{x} . The design vector \mathbf{x} is made of the spacecraft design parameters, the initial conditions at the sphere of influence and on the angle of attack:

$$\mathbf{x} = [v, \beta, \alpha, S, C_{d0}, R_b]^T \quad (10)$$

and is defined on a domain D . All feasible solutions must guarantee that the heat flux and the load factors remain for the entire atmospheric phase below q_{\max} and n_{\max} respectively.

Here uncertainties in the value of atmospheric density are considered epistemic due to a lack of information about the system. On the other hand uncertainties on the state vector at the sphere of influence can be regarded either as aleatory, if an accurate orbit determination is performed, or as epistemic during the preliminary design phase. Other sources of uncertainties related to spacecraft system parameters, as shape, geometry, mass and heat flux resistance, are considered to be epistemic. Here it is assumed that the uncertainty in the geometric and aerodynamic parameters are not directly correlated.

Problem 1:

In the first problem incoming conditions are affected by a certain level of uncertainty. A tracking station gives two intervals of values for the incoming velocity with probabilities reported in Tab.1. In the same way, for the atmospheric density two different models prescribe different set of values within a given range.

The aim is to optimise design parameters S, C_{d0}, R_b and the control parameter β , in order to maximise the belief of being in the aerocapture corridor $Bel_{ra}(r_a[r_{amin}, r_{amax}])$, i.e. the apocentre radius r_a at the exit point from the

atmosphere must be within a given range of values in order to avoid either re-entry or escape. In addition the manoeuvre must minimise the total $\Delta v = \Delta v_1 + \Delta v_2$ required to correct the final orbit. Problem (9) then becomes:

$$\mathbf{F}(\mathbf{x}) = \begin{cases} \Delta v_1 + \Delta v_2 \\ 1 - Bel_r(Y_{[r_{min}, r_{max}]}) \\ 10 - \sigma \end{cases} \quad (11)$$

$$\text{subject to } c_h \sqrt{\frac{\rho}{R_n}} v^3 \leq q_{\max}; \quad n \leq n_{\max} \quad (12)$$

where n is the g-load during the atmospheric leg and c_h has the typical value $1.89e-8$ if the heat flux is expressed in W per cm^2 [5]. The design state vector is made up of a subset of the general design vector (10) plus what could be considered the design margin σ .

$$\mathbf{x} = [\beta, S, C_{d0}, R_b, \sigma]^T \quad (13)$$

The parameter R_b is the ratio between the nose tip radius R_n and the radius of the reference frontal surface R_s . The design margin is then multiplied times the interval of uncertainty on the entry conditions and is included in the objective vector.

Table 1. Ranges of uncertain quantities for problem 1

Parameter	BPA ₁	BPA ₂
$\delta H/H$	0.1 [-0.02 0.05]	0.9 [0 0.05]
$v(km/s)$	0.1 [2.75 2.77]	0.9 [2.76 2.77]
$\delta\beta$	1 [-1e-4 1e-4]	-
ρ_0	0.1 [-0.1 0.1]	0.9 [0 0.2]

For each design vector \mathbf{x} an angle of attack α is computed in order to allow aerocapture. The angle of attack depends on the aerodynamics of the spacecraft and here it has been constrained to assume values in the interval $[-30^\circ, 30^\circ]$. For too shallow entry conditions the spacecraft must fly at maximum lift down while for too deep entry conditions the spacecraft must fly at maximum lift-to-drag ratio. Notice that the bpa associated to the control variable β , for this test case, has been set to 1 although in practise a probability of 0.99 would better represent an aleatory error.

Due to the uncertainties in the design parameters and initial states constraint equations (12) are substituted with a condition on the belief that constraints are always satisfied for any aerocapture manoeuvre:

$$Bel(q \leq q_{\max}) > 0.99; \quad Bel(n \leq n_{\max}) > 0.99; \quad (14)$$

the q_{max} is taken equal to 100 W/cm² and the maximum load factor n_{max} is fixed at 5g

Problem 2:

Test problem 2 is similar to test problem 1 but this time also the drag coefficient and the maximum bearable heat flux are affected by a level of uncertainty. The flight path angle is no more a control variable and the density at zero altitude is considered sufficiently known. The design state vector in this case is given by:

$$\mathbf{x} = [S, C_{d0}, R_b, \sigma]^T \quad (15)$$

while uncertain parameters are given in Table 2. Notice how the designer puts more confidence in a C_{d0} higher than the nominal value while for the heat flux confidence is toward a less performing heat shield.

Table 2. Ranges of uncertain quantities for problem 2

Parameter	BPA ₁	BPA ₂
$\delta H/H$	0.1 [-0.02 0.05]	0.9 [0 0.05]
$\delta v/v$	1 [2.76 2.77]	-
$\delta \beta$	1 [7.0597e-003- $\pi/2$ 7.1418e-003- $\pi/2$]	-
C_{d0}	0.2 [-0.1 0]	0.8 [0 0.1]
q_{max} (W/cm ²)	0.3 [150 300]	0.7 [80 150]

As in the previous case the objective functions are defined by equation (11) and constraints by equation (14).

5. OPTIMISATION APPROACH

The proposed optimisation approach is composed of a stochastic and a systematic step. The stochastic step is performed using an evolution strategy and is meant to obtain information on the possible presence of optima in a subdomain $D_i \subseteq D$. The systematic step is performed through a branching approach and is used to partition the domain D into subdomains D_i , where the presence of an optimum is expected. This particular hybridization can be seen as a form of niching that forces different populations to co-evolve in subregions and to form different species. This is the first difference with respect to usual global techniques. Other peculiarities of this approach relies on the way each individual explores the solution space throughout an environment-perception mechanism. The search is performed by a number of agents (explorers): each solution \mathbf{x} is associated to an agent, and is represented by a string, of length n , containing in the first m components integer values and

in the remaining s components real values. This particular encoding allows the treatment of problems with a mixed integer-real data structure. A hypercube \mathbf{S} enclosing a region of the solution space surrounding each agent, is then associated to \mathbf{x} . The solution space is then explored locally by acquiring information about the landscape within each region \mathbf{S} and globally by a portion of the population, which is continuously regenerated forming a pool of potential explorers. Each agent can communicate its findings to the others in order to evolve the entire population towards a better status. During the evolutionary step a discoveries-resources balance is maintained: a level of resources is associated to each agent and is reduced or increased depending of the number of good findings of the agent. If many agents are intersecting their migration regions and their reciprocal distance falls down below a given threshold, a repelling mechanism is activated. The threshold is a function of the number of crowding agents and a best-in-worst-out rule is used to select the repelled agent (for a comparison with known methods the interested reader can refer to [8] and [9]).

5.1 Constraint Handling Technique

The algorithm described solves bound-constrained problems but since in most of the cases, constraints are nonlinear, an extension of the algorithm has been developed in order to take into account nonlinear inequality constraints.

At each evolution step the population of solutions is divided into two subpopulations and a different objective function is assigned to each one, namely one subpopulation aims at minimising the original objective function while the other aims at minimising the residual on the constraints defined as:

$$\min_{\mathbf{y} \in D} f(\mathbf{y}) = \sum_{j=1}^q e^{R_j} \quad (16)$$

where q is the number of violated constraints and R_j is the residual of the j -th violated constraints. The two subpopulations are evolved in parallel and individuals are allowed to jump from one population to the other, i.e. if a feasible individual becomes infeasible it is inserted in the subpopulation of infeasible individuals and assigned to the solution of problem (16), on the other hand if an infeasible individual becomes feasible it is inserted in the population of feasible individuals and allocated to the minimisation of the original bound constrained objective function f . As a result the final optimal solution either is feasible or minimises infeasibilities. This procedure does not maintain feasibility for any individual, therefore once a feasible set has been found the perception mechanism is used to ensure that every move maintains the feasible population inside the feasible set. If f^* is the value of the

objective function of an individual \mathbf{y} inside the feasible set, the objective function of a new individual generated from \mathbf{y} is then augmented in the following way:

$$\min_{\mathbf{y} \in D} f = \begin{cases} f^* & \text{if every } R_j \leq 0 \\ f^* + \max \mathbf{R} & \text{if any } R_j > 0 \end{cases} \quad (17)$$

The described strategy co-evolving two populations with two different goals, allows a flexible search for feasible optimal solutions: in fact through the described use of the perception mechanism feasibility can be enforced on all feasible solutions. In this case the exploration of the solution space may be over penalised reducing the convergence rate. Therefore in order to search more extensive along the boundary of the feasible region a subset of the feasible solutions is allowed to temporary violate the constraint while preserving the feasibility of at least the best solution.

5.2 Nondominated Sorting

The multiobjective optimisation algorithm is based on the Pareto dominance of the individuals. Each feasible solution is compared with the entire population and a dominance index I_d is associated to the solution according to:

$$\begin{aligned} \text{if all } F^i(k) > F^j(k) &\Rightarrow I_d^i = I_d^j + 1 \\ \text{for } k = 1, \dots, m \text{ and } j = 1, \dots, N_p \end{aligned} \quad (18)$$

where m is the dimension of \mathbf{F} , and N_p is the number of individuals. For a reduced set of individuals using the perception mechanism to explore the solution space a strict dominance is used:

$$\begin{aligned} \text{if any } F^i(k) > F^j(k) &\Rightarrow \tilde{I}_d^i = \tilde{I}_d^j + 1 \\ \text{for } k = 1, \dots, m \text{ and } j = 1, \dots, n_p \end{aligned} \quad (19)$$

where n_p is the number of evaluations performed by an individual i in the neighbourhood space contained in \mathbf{S}^i plus the individual itself. Anyway this generates a set of nondominated individuals. A further selection is then performed by giving to each individual a reward dependent on how far has travelled in the solution space from the parent individual. Then all individuals are ranked according to their dominance index. Unlike usual population-based mechanisms that drive the entire population to cover the Pareto front, this mechanism induces the agents to *crawl* along the Pareto front.

6. RESULTS

The multiobjective optimisation process yields a front of solutions. Due to the discontinuities introduced by evidence theory and by the optimisation of the angle of

attack the distribution of solutions with a given belief is not continuous.

Notice how, for problem 1, a consistent set of solutions have a *Bel* almost equal to 1 with a corresponding low Δv cost and a large σ (see Fig.3). In this case a subset of superoptimal solutions with maximum *Bel* can be clearly identified. On the other hand, for problem 2, the number of superoptimal solutions is limited and for a reduced σ (see Fig.4). This is indeed reasonable since in the former case β could be chosen optimally. In the two figures we reported also all the solutions with *Bel* equal to zero. Notice that these solutions have anyway a non-zero *PI*.

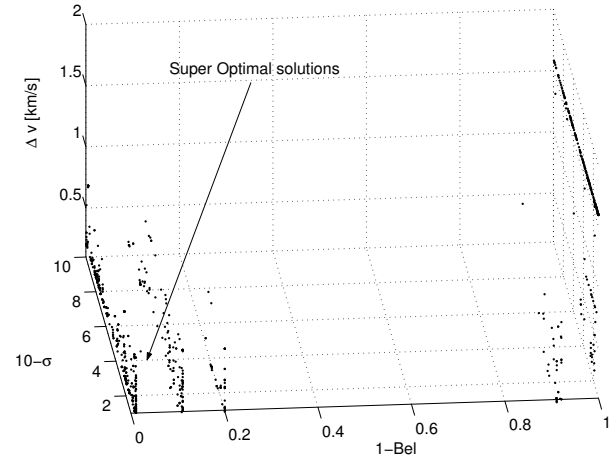


Fig 3 Solution Distribution for problem 1

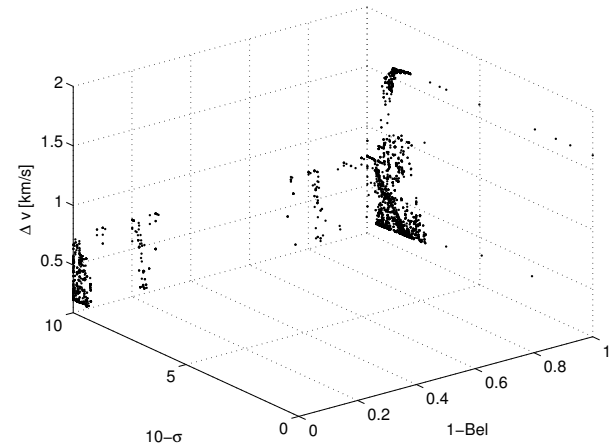


Fig. 4 Solution Distribution for problem 2

In Fig.5 and 6 some design parameters and the entry corridor for problem 1 are represented respectively. Notice how the optimal C_{d0} seems to be between 0.2 and 0.4 for all possible σ . The entry flight path angle, defining the entry corridor, is measured at 125km of altitude. The maximisation of σ allows to have almost 7 degrees of entry corridor with a minimum cost of about 0.2 km/s.

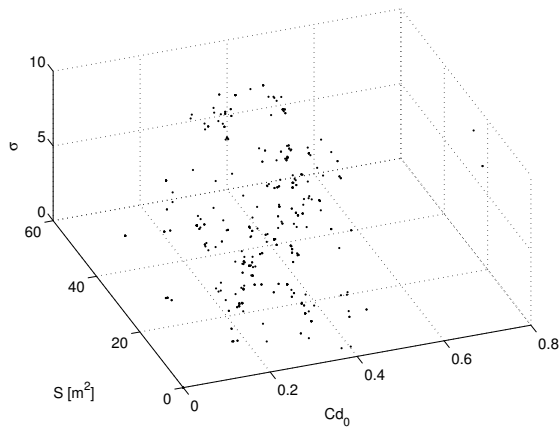


Fig. 5 Design parameters vs. uncertainty margin

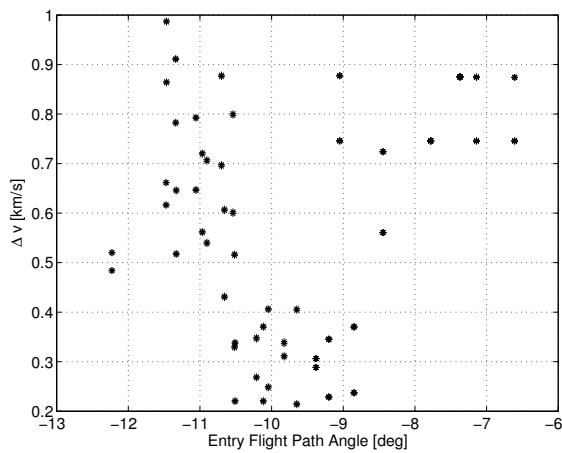


Fig. 6 Predicted corridor for problem 1

6.1 Monte Carlo verification of the results

In order to assess the robustness of the solution found in the test case, a Monte Carlo simulation has been performed taking a sample design vector and perturbing the uncertain quantities within the given ranges. A total of 300 samples have been taken and the results

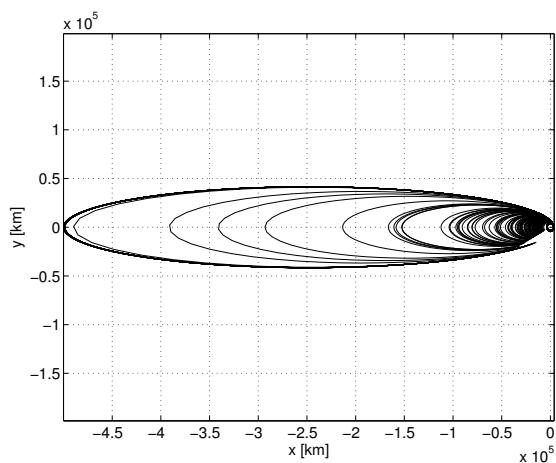


Fig. 7 Apocentre distribution for an optimised solution

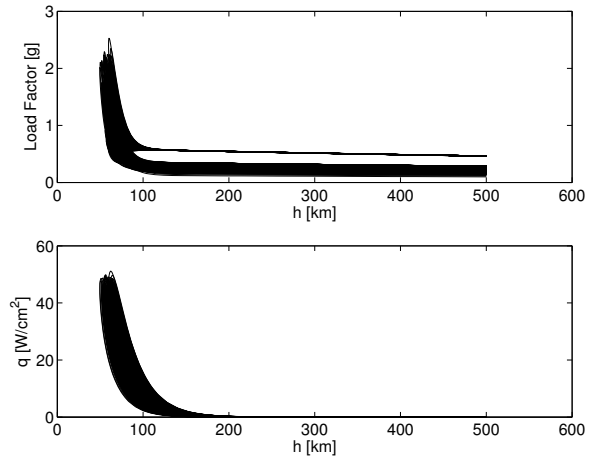


Fig. 8 Heat flux and load factor distribution

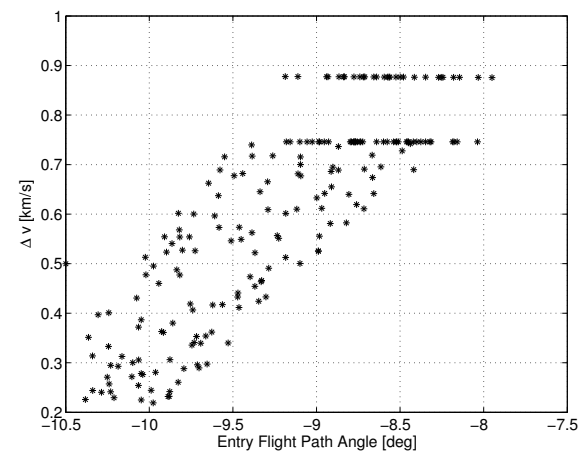


Fig. 9. Flight path angles at 125 km vs. corrective Δv

As can be seen in figures from 7 to 9, the test confirms that the selected solution is robust against perturbation of the uncertain quantities. In particular both the prediction of the total Δv and of the entry corridor are correct and the constraints are always satisfied.

7. FINAL REMARKS

In this paper a method for robust preliminary design of aerocapture trajectory. The proposed approach combines the effectiveness of evidence theory at modelling both epistemic and aleatory uncertainty on design parameters and initial conditions, with a novel co-evolutionary strategy.

Two simple examples have demonstrated how to design an aerocapture trajectory defining some system parameters, shape, aerodynamics characteristics, etc... even when uncertain information are available. The obtained solution is both Δv efficient and robust against variations of the design parameters and model data, assuring capture within the ranges of the uncertain quantities.

8. REFERENCES

1. Oberkampf W.L., Helton J.C. Investigation of Evidence Theory for Engineering Applications. AIAA 2002-1569, 4th Non-Deterministic Approaches Forum, 22-25 April 2002, Denver, Colorado.
2. Agarwal H., Renaud J., Preston E. Trust Region Management Reliability Based Design Optimization Using Evidence Theory. AIAA-2003-1779, 5th AIAA Non-deterministic Approaches Forum, AIAA/ASME/ASCE/AHS/ASC Structures, Structural Dynamics and Materials Conference, Norfolk, Virginia, Apr. 7-10, 2003.
3. Helton J.C., Oberkampf W.L., Johnson J.D. Competing Failure Risk Analysis Using Evidence Theory. AIAA 2003-1911, AIAA/ASME/ASCE/AHS, Structures, Structural Dynamics and Materials Conference, Norfolk, Virginia, Apr. 7-10, 2003
4. Rousseau S., Perot E., Graves C., Masciarelli J.P., Queen E. Aeroacapture Guidance Algorithm Comparison Campaign. AIAA-2002-4822.
5. Mitcheltree R.A., DiFulvio M., Horvath T.J., Braun R.D. Aerothermal Heating Predictions for Mars Microprobe. Journal of Spacecraft and Rockets Vol.36, No.3, May-June 1999.
6. Regan F.J., Anandkrishnan S.M. Dynamics of Atmospheric Re-entry. AIAA Educational Series 1993.
7. Larson W. J., Pranke L.K. Human Spaceflight Mission Analysis and Design. McGraw-Hill.
8. Vasile M. A Systematic-Heuristic Approach for Space Trajectory Design. Astrodynamics, Space Missions and Chaos, Ann NY Acad Sci 2004 Vol. 1017:234-254.
9. Vasile, M, Summerer, L., De Pascale, P., Design of Earth-Mars Transfer Trajectories using evolutionary branching technique, IAC-03-A.7.07, 54th International Astronautical Congress, 29 September-3 October 2003, Bremen, Germany